

# Magnetoresistance and electrical hysteresis in stable half-metallic $\text{La}_{0.7}\text{Sr}_{0.3}\text{MnO}_3$ and $\text{Fe}_3\text{O}_4$ nanoconstrictions

O. Céspedes,<sup>a)</sup> S. M. Watts,<sup>b)</sup> and J. M. D. Coey  
 Physics Department, CRANN, Trinity College, Dublin 2, Ireland

K. Dörr  
 IFW Dresden, Postfach 270016, D-01171 Dresden, Germany

M. Ziese  
 Superconductivity and Magnetism division, University of Leipzig, 04103 Germany

(Received 29 December 2004; accepted 28 June 2005; published online 15 August 2005)

We have studied the transport properties of mechanically stable  $\text{Fe}_3\text{O}_4$  and  $\text{La}_{0.7}\text{Sr}_{0.3}\text{MnO}_3$  nanoconstrictions patterned by focused ion-beam milling. The magnetoresistance decreases with the square of the applied voltage and scales with the resistance of the constriction, with values up to 8000% for magnetite and 100% for  $\text{La}_{0.7}\text{Sr}_{0.3}\text{MnO}_3$ . These results are interpreted within a model for domain-wall magnetoresistance. Some samples exhibit electrical hysteresis with discrete changes of resistance that disappear in the presence of a magnetic field, indicating domain-wall displacement driven by a spin-polarized current. © 2005 American Institute of Physics.  
 [DOI: 10.1063/1.2011770]

$\text{Fe}_3\text{O}_4$  (magnetite) and  $\text{La}_{0.7}\text{Sr}_{0.3}\text{MnO}_3$  (LSMO) are ferromagnets with high spin polarization at room temperature, which makes them two interesting candidates for devices based on spin transport. However, most of the work done on magnetic transport across nanoconstrictions has been carried out with 3d ferromagnetic metals, mainly nickel.<sup>1–4</sup> Exceptions are the studies of magnetoresistance performed in point contacts of ferromagnetic oxides such as  $\text{Fe}_3\text{O}_4$ , LSMO, and  $\text{CrO}_2$  (Refs. 5 and 6). However, point contacts present mechanical issues such as magnetostriction.<sup>7–9</sup> They degrade in a few minutes and therefore offer no prospects for applications.

Here we present electrical measurements carried out on  $\text{Fe}_3\text{O}_4$  and LSMO nanostructures patterned by focused ion beam (FIB) on films 50–150 nm thick [Fig. 1(a)]. These patterned nanostructures which are bonded to a substrate are mechanically stable. Magnetostrictive effects are minimized, and potential applications can be envisaged. Study of transport through these structures may give some insight into the passage of a highly spin-polarized current across a narrow domain wall.

The  $\text{Fe}_3\text{O}_4$  films were grown by reactive dc-magnetron sputtering in oxygen atmosphere from a pure Fe target onto  $\text{MgO}$  (001) or  $\text{Al}_2\text{O}_3$  (001) substrates. Magnetite films on  $\text{MgAl}_2\text{O}_4$  and all the LSMO films were grown by pulsed laser deposition from stoichiometric, polycrystalline targets. Resistance measurements on the magnetite films show a clear Verwey transition around 120 K.

A focused ion beam can be used to pattern nanostructures with dimensions of less than 20 nm starting from a track prepared by UV lithography by removing the undesired material with accelerated  $\text{Ga}^+$  ions. The milling process can be monitored by direct observation with scanning electron microscopy (SEM) in a dual-beam system.

We have patterned single and multiple nanoconstrictions 20–50 nm wide in LSMO and  $\text{Fe}_3\text{O}_4$  [Fig. 1(b)]. A domain wall similar in size to the nanoconstriction is expected to form there in either material.<sup>10,11</sup> This implies a change of the magnetization direction over about 10 nm.

We find that the Ga/Fe atomic ratios in these nanostructures can be kept below 1 at. % if the sample imaging and positioning is made with the SEM in the dual-beam system and a silver cap layer some 60-nm thick (removed afterwards by argon milling) is used.

The  $I:V$  characteristic of our samples can be fitted to  $I = \beta(V + \gamma V^3)$ . The values for  $\beta$  (conductance) and  $\gamma$  (nonlinearity) in single and multiple nanoconstrictions are:  $\beta \sim 10^{-5}$ – $10^{-4} \Omega^{-1}$  for LSMO and magnetite,  $\gamma \sim 10^{-3}$ – $10^{-2} \text{V}^{-2}$  for magnetite, and  $\sim 0$ – $100 \text{V}^{-2}$  for LSMO. We found no difference between the transport of single and multiple nano-

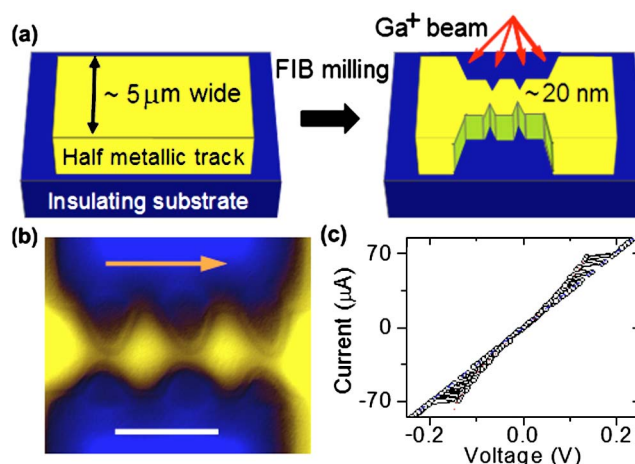


FIG. 1. (Color online) (a) Schematic of the fabrication process: focused ion-beam milling of a double nanoconstriction departing from a 5- $\mu\text{m}$  track. (b) SEM of an LSMO (bright) triple nanoconstriction where we intend to trap magnetic domain walls (the arrow points to the current direction, the scale bar is 500 nm). (c) Fluctuation between Ohmic ( $\gamma=0$ ) and tunneling ( $\gamma=15$ ) regimes in the  $I:V$  characteristic of an LSMO nanoconstriction.

<sup>a)</sup>Present address: Service de Physique de l'Etat Condensé, CEA Saclay, 91191 Gif sur Yvette cedex, France; electronic mail: cespius@yahoo.com

<sup>b)</sup>Present address: Physics of Nanodevices Group, University of Groningen.

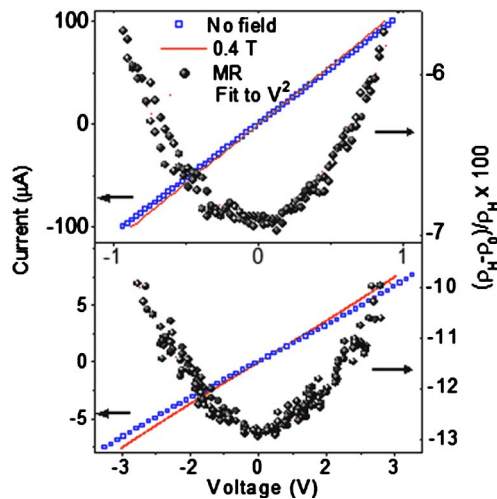


FIG. 2. (Color online) Typical  $I$  and MR vs  $V$  characteristics for a magnetite (top) and LSMO (bottom) nanoconstriction. The MR can be fitted to a  $V^2$  dependence (dotted line).

constrictions, probably because the interconstriction regions ( $\sim 0.5 \times 0.5 \mu\text{m}^2$ ) are too big to form a single-domain state.

Charging effects (Coulomb blockade) are known to produce nonlinearities in the transport across noble-metal point contacts,<sup>12</sup> and similar effects may exist for the nanostructures considered here. As in the reference, we find no correlation between  $\beta$  and  $\gamma$ . However, in the case of LSMO nanostructures, only samples with  $\beta \lesssim G_0$  ( $\equiv [12.9 \text{ k}\Omega]^{-1}$ ) show nonlinearity ( $\gamma \neq 0$ ). LSMO nanostructures with a conductivity of the order of  $G_0$  can present fluctuations between ohmic and nonlinear transport [Fig. 1(c)]. The RT characteristic of both  $\text{Fe}_3\text{O}_4$  and LSMO nanostructures with  $\gamma \neq 0$  is characteristic of localized electron behavior with an activation energy of order 0.1 eV. In consecutive  $I:V$  cycles and ac measurements up to 1 MHz, we find no evidence for electromigration or heating effects, probably because of dissipation through the substrate and the use of not-too-high current densities (always below  $5 \times 10^6 \text{ A/cm}^2$ ).

The localization is partially of magnetic origin, as evidenced by the fact that an applied magnetic field will reduce not only the resistance but also the nonlinearity of the sample. The magnetoresistance (MR) has a  $V^2$  dependence, and it saturates at field values below 0.4 T both for magnetite and LSMO nanoconstrictions (Fig. 2). The relaxation time for a sample to revert to the initial resistance after a magnetic field is applied is of the order of days, and this process is not speeded up by heating or cooling the sample. The MR is independent of the direction of the applied field both in sign and magnitude. All these characteristics, and the fact that the samples are bound to a substrate, are difficult to reconcile with a magnetomechanical or magnetostatic effect.<sup>7-9</sup>

Most of the nanoconstrictions (38/55) present little ( $<1\%$ ) or no MR. However, a significant number of nanoconstrictions and nanobridges (14/55) show a MR of 1–20% at room temperature. Only a few of the samples (3/55) show the huge MR ratios reported for electrodeposited Ni nanocontacts and half-metallic point contacts.

There is evidence that the magnetoresistance is associated with the magnetic structure in the vicinity of the nanoconstriction. The data points (Fig. 3) seem to fall on two branches: one with MR in the range 1–8000% and where the effect increases with resistance, with most of the points fall-

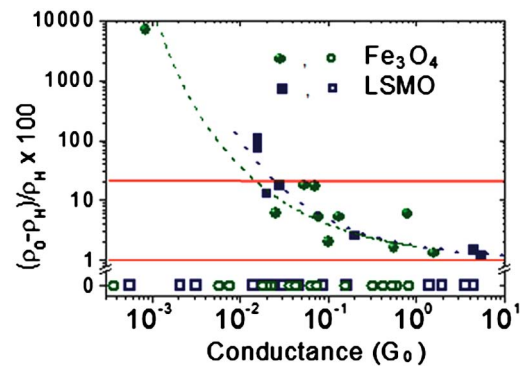


FIG. 3. (Color online) Scaling of the MR at 0 V with the conductance in units of  $G_0$  ( $\approx [12.9 \text{ k}\Omega]^{-1}$ ) for magnetite and LSMO nanoconstrictions. Open symbols give the distribution of the conductance for samples with no MR. The two lines delimit the region between 1 and 20%, where most of the results fall with MR  $>1\%$ .

ing in the 1–20% range, and the other branch with no measurable MR ( $<0.5\%$ ).

We associate one branch with the presence of a magnetic domain wall in the nanoconstriction, and the other with the absence of a wall. In the latter case there is roughly no magnetoresistance. In the former, the magnetoresistance is associated to a long recovery time ( $\sim$ days), suggesting that the wall is irreversibly moved to a new pinning site far from the constriction. The wall width is related to the size of the patterned structure at the pinning point,<sup>10,11</sup> so once the wall is moved from the narrowest point (nanoconstriction), it will expand and allow for an easier flow of electrons, reducing the resistance. The smaller the constriction, the narrower will be the domain wall and therefore bigger its contribution to the resistance. Hence the scaling of the MR with the resistance.

The long relaxation times to go back to the original high resistance are then due to the nucleation of a new domain wall at the nanoconstriction.<sup>13</sup> This time can vary compared to the bulk properties due to differences in the magnetic anisotropy and the presence of defects that act as pinning centers.

The reduction of  $\gamma$  when a magnetic field is applied could also be related to the presence of a wall at the nanostructure. The electrons may not be able to follow this sharp change of the magnetization direction through scattering,<sup>10</sup> and would then have to hop or tunnel across the wall, increasing the nonlinearity  $\gamma$ . When a magnetic field is applied the domain wall is pushed out of the nanoconstriction and the electrons can follow the magnetization by scattering across the nanoregion. The previous nonlinear transport across the wall is then transformed into a diffusive channel by a magnetic field (reducing  $\gamma$ ) and gives place to the  $V^2$  dependence of the MR.

Some nanoconstrictions present electrical hysteresis (Fig. 4). The resistance of these samples seems to vary with the current in discrete steps, forming a staircase with changes of resistance for an LSMO sample of about 1% every 1–5  $\mu\text{A}$  (Fig. 4, inset). When a magnetic field is applied, the resistance of these samples drops, and both the electrical hysteresis and discrete changes disappear.

The electrical hysteresis and discrete variations of resistance can also be explained in terms of a domain wall trapped at the nanoconstriction, which can be pushed out from there to other pinning centers in the neighborhood via a

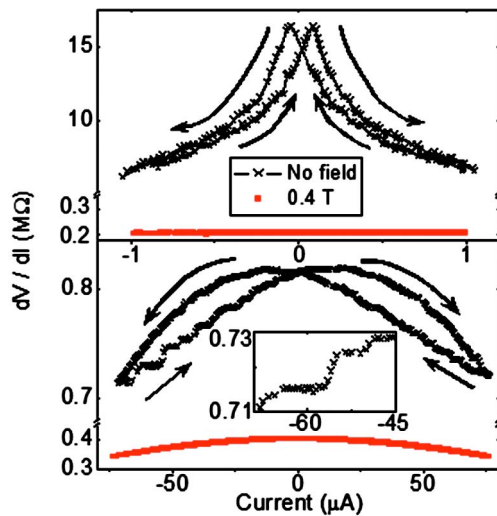


FIG. 4. (Color online)  $I:V$  characteristic before (hysteretic) and after a magnetic field is applied for a magnetite (top) and an LSMO (bottom) nanoconstriction. Inset: discrete variations of the resistance with the current.

spin-polarized current due to the phenomena known as *spin pressure*.<sup>14–16</sup> The mechanisms through which a magnetic domain wall may be displaced out of the constriction via the spin pressure are two:<sup>5</sup> (1) transfer of momentum (linear and angular) from the electrons to the atoms that form the domain wall (via diffusive scattering) and (2) the gain of energy of every hopping electron when crossing the wall without spin flip (exchange drag pressure). This energy gain when crossing the wall is equal to  $J_{dd} \cdot \sin^2 \theta / 2$  per electron, with  $J_{dd}$  the exchange energy and  $\sin^2 \theta$  the square of the sine of the angle between the directions of the spin of the electron and the magnetization of the surrounding environment. The pressure exerted by the spin-polarized current over the domain wall is:<sup>5</sup>

$$P = \frac{j}{e} \frac{\sqrt{n_{\text{hop}}}}{\nu} J_{dd} \quad (1)$$

with  $j$  the current density,  $e$  the electron charge,  $n_{\text{hop}}$  the number of hopping electrons crossing the wall, and  $\nu$  the conduction-electron velocity.

The other pinning centers, where the wall has been moved to, are in wider areas of the nanostructure, providing an expansion of the domain wall. Therefore, the resistance of the device will depend on the position of the domain wall, that is, on the currents previously applied, giving rise to a hysteretic  $I:V$  characteristic as measured in Fig. 4. The different discrete values of resistance correspond to different pinning positions of the domain wall. When a magnetic field is applied, the wall is displaced far from the constriction and it expands, reducing the spin pressure. The wall cannot then

be displaced by the current and the electrical hysteresis disappears (Fig. 4).

We have fabricated mechanically stable nanoconstrictions by UV lithography and focused ion-beam milling from half-metallic  $\text{Fe}_3\text{O}_4$  and  $\text{La}_{0.7}\text{Sr}_{0.3}\text{MnO}_3$  thin films. The nanoconstrictions provide highly resistive and nonlinear  $I:V$  characteristics, which we attribute to spin-dependent charging effects and nondiffusive transport across a magnetic domain wall trapped at the nanoconstriction. Hysteretic  $I:V$  characteristics with discrete changes in resistance are explained in terms of domain-wall displacement via the spin pressure generated by a spin-polarized current.

Because the mechanisms for domain-wall displacement depend on the net spin flow rather than on the charge flow, magnetic nanoconstrictions may be used in spin electronic devices where the position of the domain wall, and therefore their transport characteristic, is tuned by magnetic fields and pure spin currents, dissociated from the electronic charge<sup>17</sup> and therefore without the heating due to power dissipation. Multiple nanoconstriction structures could also be used as magnetic memories where the magnetization direction of the internanoconstriction region would be controlled by spin-polarized electric currents rather than by magnetic fields.<sup>5</sup>

This work was supported by Science Foundation Ireland. The authors are grateful to Dr. Alberto Bollero for the magnetite films on  $\text{MgAlO}_4$  substrates.

- <sup>1</sup>N. García, M. Muñoz, and Y. W. Zhao, Phys. Rev. Lett. **82**, 2923 (1999).
- <sup>2</sup>S. H. Chung, M. Muñoz, and N. García, Phys. Rev. Lett. **89**, 287203 (2002).
- <sup>3</sup>H. D. Chopra and S. Z. Hua, Phys. Rev. B **66**, 020403 (2002).
- <sup>4</sup>M. Viret, S. Berger, M. Gabureac, F. Ott, D. Olligs, I. Petej, J. F. Gregg, C. Fermon, G. Francine, and G. Le Goff, Phys. Rev. B **66**, 220401 (2002).
- <sup>5</sup>J. J. Versluijs, M. A. Bari, and J. M. D. Coey, Phys. Rev. Lett. **87**, 026601 (2001).
- <sup>6</sup>J. M. D. Coey, J. J. Versluijs, and M. Venkatesan, J. Magn. Magn. Mater. **226**, 688 (2001).
- <sup>7</sup>E. B. Svedberg, J. J. Mallet, H. Ettetgui, L. Gan, P. J. Chen, A. J. Shapiro, T. P. Moffat, and W. F. Egelhoff, Appl. Phys. Lett. **84**, 236 (2004).
- <sup>8</sup>W. F. Egelhoff, L. Gan, H. Ettetgui, Y. Kadmon, C. J. Powell, P. J. Chen, A. J. Shapiro, R. D. McMichael, J. J. Mallet, T. P. Moffat, M. D. Stiles, and E. B. Svedberg, J. Appl. Phys. **95**, 7554 (2004).
- <sup>9</sup>O. Céspedes, E. Clifford, and J. M. D. Coey, J. Appl. Phys. **97**, 064305 (2005).
- <sup>10</sup>P. Bruno, Phys. Rev. Lett. **83**, 2425 (1999).
- <sup>11</sup>Y. Labaye, L. Berger, and J. M. D. Coey, J. Appl. Phys. **91**, 5341 (2002).
- <sup>12</sup>J. L. Costa-Krämer, N. García, P. García-Mochales, P. A. Serena, M. I. Marqués, and A. Correia, Phys. Rev. B **55**, 5416 (1997).
- <sup>13</sup>M. H. Jo, N. D. Mathur, and M. G. Blamire, Appl. Phys. Lett. **80**, 2722 (2002).
- <sup>14</sup>M. Klaui, C. A. F. Vaz, J. A. C. Bland, W. Wernsdorfer, G. Faini, E. Cambril, and L. J. Heyderman, Appl. Phys. Lett. **83**, 105 (2003).
- <sup>15</sup>E. B. Myers, D. C. Ralph, J. A. Katine, R. N. Louie, and R. A. Buhrman, Science **285**, 867 (1999).
- <sup>16</sup>G. Tatara and H. Kohno, Phys. Rev. Lett. **92**, 086601 (2004).
- <sup>17</sup>T. P. Parek, Phys. Rev. Lett. **92**, 076601 (2004).